



## The impacts of recent drought and fire in lowland Bolivia on forest loss and regional smoke emissions

Joshua P. Heyer<sup>1</sup>, Mitchell J. Power<sup>1,2</sup>, Robert D. Field<sup>3,4</sup>, and Margreet J.E. van Marle<sup>5,6</sup>

<sup>1</sup>Geography Department, University of Utah, Salt Lake City, UT 84112-9155, USA

5 <sup>2</sup>Natural History Museum of Utah, University of Utah, Salt Lake City, UT 84112, USA

<sup>3</sup>NASA Goddard Institute for Space Studies, New York, NY 10025, USA

<sup>4</sup>Department of Applied Physics and Applied Mathematics, Columbia University, New York, NY 10025, USA

<sup>5</sup>Faculty of Earth and Life Sciences, Vrije Universiteit Amsterdam, Amsterdam, Netherlands,

<sup>6</sup>Deltares, Delft, the Netherlands

10 *Correspondence to:* Joshua P. Heyer ([josh.heyser@geog.utah.edu](mailto:josh.heyser@geog.utah.edu))

**Abstract.** In the southern Amazon relationships have been established among drought, human activities that cause forest loss, fire, and smoke emissions. We explore the effects of recent drought on fire, forest loss, and atmospheric visibility in lowland Bolivia. To assess human influence on fire, we consider climate, fire and vegetation dynamics in an area largely excluded from human activities since 1979, Noel Kempff Mercado National Park (NK) in northeastern Bolivia. We use data  
15 from five sources: the Moderate Resolution Imaging Spectroradiometer Collection 6 active fire product (2001–2015) (MODIS C6), Global Fire Weather Database data (1982–2015) (GFWED), MODIS land-cover data (2001–2010), MODIS forest loss data (2000–2012), and extinction coefficient derived from horizontal visibility data from the World Meteorological Organization (WMO)-level surface stations (1973–2015), which is affected by smoke and acts as a proxy for regional fire activity. In lowland Bolivia from 2001–2015, interannual Drought Code (DC) variability was linked to fire  
20 activity, while from 1982–2015, interannual DC variability was linked to  $B_{\text{ext}}$  visibility data. From 2001–2015, the regional extinction coefficient for the southwestern Amazon  $B_{\text{ext}}$  and MODIS C6 active fire data for lowland Bolivia captured fire seasonality, and covaried between low and high fire years. Consistent with previous studies, our results suggest the extinction coefficient  $B_{\text{ext}}$  can be used as a longer-term proxy of regional fire activity in southwestern Amazonia. Overall, our study found drought conditions were the dominant control on interannual fire variability in lowland Bolivia, and fires  
25 within NK were limited to the cerrado and seasonally-inundated wetland biomes. Our results suggest lowland Bolivia tropical forests were susceptible to human activities that may have amplified fire during times of drought. Human activities



and drought need to be considered in future projections of southern Amazonia fire, in regard to carbon emissions and global climate.

## 30 **1 Introduction**

Observations from the southern Amazon reveal fire emissions increased from 1987 through the early 2000s (van Marle et al., 2017). During this time, humans used fire in the southern Amazon while logging timber, and to clear land for building infrastructure and agriculture (Moran, 1993; Nepstad et al., 1999; Fearnside, 2005; Morton et al., 2008; Cochrane, 2009; Nepstad et al., 2009; van der Werf et al., 2010), suggesting human activities had a significant impact on increased smoke  
35 emissions from fire (van Marle et al., 2017). To reduce the impacts of deforestation and fire on forest loss in the southern Amazon, and in turn on carbon emissions and global climate, incentives and policies were implemented in the early 2000's (Nepstad et al., 2009; Hansen et al., 2013). While these policy changes have eased deforestation rates in areas of the Brazilian Amazon (Nepstad et al., 2009; Hansen et al., 2013), forest loss from deforestation and fire has continued in parts of the southern Amazon, particularly in lowland Bolivia (Chen et al., 2013b; van Marle et al., 2016; van Marle et al., 2017).  
40 Likely amplifying the effects of deforestation and fire on forest loss in the southern Amazon were drought conditions during the early 2000s (Brown et al., 2006; Aragão et al., 2007; Marengo et al., 2008), raising the question, what are the relationships among recent drought, fire and forest loss in lowland Bolivia?

Both paleofire investigations (Bush et al., 2008; Marlon et al., 2008; Power et al., 2013) and modern fire records (Brown et al., 2006; Aragão et al., 2007; Marengo et al., 2008) link drought to fire in the southern Amazon. Our study considers  
45 relationships between recent drought and fire in lowland Bolivia using the Global Fire Weather Database (GFWED) (Field et al., 2015) and the Moderate Resolution Imaging Spectroradiometer collection 6 (MODIS C6) active fire product (Giglio et al., 2016). The GFWED Drought Code (DC) in particular captures net drying of deep fuels, with lower DC values observed during the wet season and higher DC values during the dry season (Field et al., 2015). We use the DC as an indicator of antecedent dry (wet) conditions during the wet and dry seasons, which influence high (low) DC values during the following  
50 fire season from August–October in lowland Bolivia.

In addition to understanding links between drought and fire in lowland Bolivia, we also consider where past fires occurred spatially in relation to land use and biome type using data from the MODIS-based global land cover product



(Broxton et al., 2014), and the Landsat-based forest loss product (Hansen et al., 2013). Considering humans have had a significant impact on forest loss and fire activity in unprotected biomes, we compare fire distribution in unprotected biomes  
55 in lowland Bolivia to biomes in Noel Kempff Mercado National Park (NK), an area in lowland Bolivia protected from deforestation since 1979. Specifically, we explore climate and fire relationships in NK to determine when fire activity is high in relation to interannual climate variability, and where fire occurs spatially in relation to different biomes and land uses.

Finally, to extend our fire record for lowland Bolivia prior to the onset of MODIS C6 in 2001, we analyze horizontal visibility data from World Meteorological Organization (WMO) level surface weather stations. Visibility data has been used  
60 as a fire emissions proxy to understand fire activity over the southern Amazon from 1973–2015 (van Marle et al., 2017). We test relationships between MODIS C6 active fire data for lowland Bolivia and regional WMO-visibility data (locations of weather stations in Fig. 1a), to determine how well visibility data corresponds to the MODIS C6 fire record from 2001–2015, and to extend the fire record for lowland Bolivia prior to 2001.

Our results are useful and relevant when considering uncertainties regarding the fate of the southern Amazon in  
65 response to climate change (Zhang et al., 2015). Here, we show how recent interannual climate variability has impacted fire activity across different biomes in lowland Bolivia. Valuable results when considering in the southern Amazon fire weather (Bedia et al., 2015) and fire season severity are expected to increase during the 21<sup>st</sup> century (Flannigan et al., 2013), which could impact carbon emissions and global climate (Fearnside, 2005; Aragão et al., 2014).

## 70 2 Methods and Data

### 2.1 MODIS C6 and Landsat Data

The Moderate Resolution Imaging Spectroradiometer Collection 6 active fire product (MODIS C6) offers a tool to adequately answer questions related to recent fire activity from 11/2000–present (Morton et al., 2011). MODIS C6 has been  
75 used globally to explore a variety of fire related questions ranging from biomass burning (Wooster et al., 2003) and fire detection in the Amazon (Chen et al., 2013a). High-spatial resolution (500 meter) near real time MODIS C6 data used in our analyses are provided by the Land, Atmosphere Near real-time Capability for Earth Observing System Fire Information for Resource Management System, and operated by the NASA/Goddard Space Flight Center/Earth Science Data and Information System (Giglio et al., 2016). Two key limitations of the previous MODIS C5 product were small forest clearings



80 causing false active fires, and thick smoke obscuring large fires (Giglio et al., 2016). For tropical ecosystems, these two key limitations were addressed and errors were reduced from MODIS C5 to MODIS C6 (Giglio et al., 2016).

For our study, MODIS C6 data for Bolivia (Fig. 1b) was downloaded using the NASA Earth Observation Data archive download tool. Data was subset by location (e.g., NK), year and by fire detection confidence  $\geq 90\%$ . Only active fire points  $\geq 90\%$  were included in our analyses to further reduce the potential for false active fires. MODIS C6 data seen in Brazil are  
85 shown in spatial analyses (i.e., Fig. 4 and 5), but were not used in statistical analyses (Tables 1, 2, 3).

MODIS based Collection 5.1 MCD12Q global land cover data (Broxton et al., 2014) and Landsat forest loss data 2000–2012 (Hansen et al., 2013) were obtained to determine the spatial coherency of fire, land use, and forest loss. MODIS land-cover types seen in figure legends (e.g., Figs. 1b) will be referred to in the paper hereafter as the cerrado, METF, SDTF, and seasonally inundated wetlands. Cerrado biome land cover types are open shrublands, woody savannas, savanna, and  
90 grasslands. SDTF biome land-cover types are deciduous needleleaf forest, deciduous broadleaf forest, mixed forest, and closed shrublands. The METF biome includes the evergreen broadleaf forest MODIS land-cover type. The seasonally inundated wetland biome includes the permanent wetland and grasslands MODIS land-cover types.

## 2.2 Horizontal Extinction Coefficient calculated from Visibility Observations

95 In the absence of long-term fire data, horizontal visibility has been used as a proxy for fire activity in Indonesia (Field et al., 2009; Field et al., 2016) and Amazonia (van Marle et al., 2017). Here, horizontal visibility observations (1973–2015) were taken from the NOAA National Climatic Data Center Integrated Surface Database (<https://catalog.data.gov/dataset/integrated-surface-global-hourly-data>), which is comprised of data from WMO-level surface stations provided by national meteorological agencies. Horizontal visibility observations are human-made using landmarks  
100 with known distances during the day and using point light sources at night (World Meteorological Organization, 1996). Horizontal visibility is influenced by several sources including dust, air pollution, haze, fog, and precipitation. Fires also have a strong impact on visibility, and therefore is used here as a proxy of regional fire activity in lowland Bolivia.

To correct for limitations of the human eye and imperfections of the landmarks used to estimate the maximum distance seen, the observations in meters are usually expressed as the extinction coefficient ( $B_{\text{ext}}$ ,  $\text{km}^{-1}$ ). In our case,  $B_{\text{ext}}$  corresponds  
105 to the degree to which light is attenuated by scattering and extinction over a horizontal path. Eleven stations were selected



and the monthly median  $B_{\text{ext}}$  over these selected stations was found representative for fire emissions over the region (7°S–17°S, 58°W–68°W) (Fig. 1a). We only used individual observations taken at 12:00 UTC (corresponding to 08:00 local time), as the frequency of reports at other times varied considerably during the length of record. The data were subsequently filtered following Husar et al. (2000) and van Marle et al. (2017) to omit observations influence by fog or precipitation, and aggregated to monthly values.

### 2.3 Global Fire Weather Database

To examine climatic controls on fires in NK, we used weather parameters and components of the Fire Weather Index (FWI) System, which integrates different surface weather parameters influencing the likelihood of fires starting and spreading. The FWI System consists of moisture codes for three generalized fuel classes and three fire behavior components, computed each day from surface temperature, relative humidity (RH), wind speed and precipitation. Because of its flexibility, it is the most widely used such system in the world, and has been adapted for use in different fire environments operationally and for research purposes (de Groot and Flannigan, 2014).

To explore interannual climate variability related to fire activity in lowland Bolivia, FWI data for period 1982–2015, were obtained from the Global Fire Weather Database (GFWED) (Field et al., 2015), and processed for a 50 km x 50 km bounding box over NK (13°S x 15.3°S, 62.2°W x 59.5°W), and for a bounding box over lowland Bolivia. The GFWED, gridded to a 0.5° latitude x 2/3° longitude resolution, includes different versions that are all computed using temperature, RH and wind speed from the NASA MERRA2-reanalysis (Gelaro et al., 2017), but using different estimates of daily precipitation, which is the most uncertain input to the FWI system, particularly in the tropics (Field et al., 2015). From these, we use in our analyses the Drought Code (DC), along with precipitation (mm/day), temperature (C°), and RH (%). The DC is an indicator of seasonal drying (Field et al., 2015), and is the simplest of the six FWI components. DC values that exceed 425 are considered extreme (Field et al., 2015). Precipitation, temperature and RH were included to compare the explanatory power of basic surface weather variables compared to the DC. For the DC and precipitation, we used versions computed from the ‘raw’ MERRA2 precipitation estimate and a MERRA2 rain gauge-corrected version used in the MERRA2 land surface scheme, to provide a measure of the dependence of our results on uncertainty in the precipitation estimates.

Additional precipitation data were obtained from the Climate Prediction Center (CPC), the Global Precipitation Climatology



Project (GPCP), and the Tropical Rainfall Measuring Mission (TRMM). The CPC estimates precipitation from rain gauge data at  $0.5^\circ \times 0.5^\circ$  resolution (Chen et al., 2008), the GPCP estimated precipitation from satellites at  $2.5^\circ \times 2.5^\circ$  resolution (Huffman et al., 2009), and the TRMM estimated precipitation from satellites at  $0.25^\circ \times 0.25^\circ$  resolution (Huffman et al., 135 2007). For each GFWED variable, mean monthly time series were constructed for Bolivia and NK from 01/2001–12/2015, and from 01/1982–12/2015. Mean-fire season (August – October) time series were also created for selected GFWED variables from 08/1982–10/2015.

## 2.5 Statistical Analyses

140 Several sets of linear correlations were performed in R to better understand relationships among MODIS C6, GFWED and WMO-visibility data. For each set of correlations, correlation coefficients were estimated among monthly MODIS C6 data and mean-monthly GFWED and WMO-visibility data using a Pearson's coefficient, with a standard transformation to a t-statistic to assess significance (e.g., alpha level: 0.05). Finally, to extend the fire record prior to 2001, correlations for lowland Bolivia were performed between mean fire season (i.e., August–October) GFWED variables and  $B_{\text{ext}}$  data from 145 01/1982–12/2015.

## 3 Results

### 3.1 Fire spatial distribution and seasonality in lowland Bolivia and NK (2001–2015)

The spatial distribution of MODIS C6 active fires in lowland Bolivia and NK are seen from 2001–2015 (Fig. 1b). For 150 lowland Bolivia from 2001–2015, a significant relationship was found between mean-monthly MODIS C6 fire data and  $B_{\text{ext}}$  data, with a 95% correlation confidence interval of 0.76–0.86. During this time 85% of mean-monthly MODIS C6 fires were from August–October, with an average of 10,574 fires/year (Fig. 2a). Both MODIS C6 fire seasonality and peak  $B_{\text{ext}}$  occurred from August–October. For NK from 01/2001–12/2015, 96% of mean-monthly MODIS C6 fires were from August–October, with an average of 65 fires/year (Fig. 2b).

155

### 3.2 Climate and fire relationships in lowland Bolivia

For lowland Bolivia from 2001–2015, higher-than-normal (i.e.,  $> 10,574$  fires/year) MODIS C6 fire years were identified in 2004, 2005, 2007, 2008, 2010, and 2011 (Fig. 3a). Relationships among Bolivia monthly MODIS C6 fire data and mean-



monthly GFWED precipitation (Fig. 3b) and temperature (Fig. 3d) variables were weaker than relationships among Bolivia  
160 monthly MODIS C6 fire data and mean-monthly GFWED relative humidity and DC variables (Table 1; Fig. 3c, e).  
However, statistical relationships among Bolivia monthly MODIS C6 fire data and mean-monthly GFWED temperature and  
precipitation variables were still significant.

Inverse relationships between MODIS C6 and precipitation across MERRA2, CPC, GPCP and TRMM were all  
comparably low (Table 1). Of the precipitation sources analyzed, the strongest observed relationship was between Bolivia  
165 MODIS C6 and MERRA 2 precipitation data, with a 95% correlation confidence interval of -0.27 – -0.51. A significant  
inverse relationship was observed between MODIS C6 active fire data and MERRA2 relative humidity, with a 95%  
correlation confidence interval of -0.56 – -0.73 for lowland Bolivia. Next, a positive relationship can be seen between  
MODIS C6 active fire and MERRA2 temperature data, with a 95% correlation confidence interval of 0.43 – 0.64. Finally,  
stronger relationships were observed among MODIS C6 active fire data and TRMM DC, GPCP DC, and CPC DC, when  
170 compared to correlations between MODIS C6 active fire data and MERRA2 DC. The strongest relationship for DC was  
between Bolivia MODIS C6 data and GPCP DC, with a 95% correlation confidence interval of 0.69 – 0.82.

### 3.3 Climate and fire relationships in NK

For NK from 2001–2015, higher-than-normal (i.e., > 65 fires/year) MODIS C6 active fire years were identified in 2003,  
175 2004, 2005, 2007, 2010, and 2012 (Fig. 3f). Significant relationships were found among monthly NK MODIS C6 active fire  
data and mean-monthly GFWED variables for NK (Table 1). Relationships among monthly NK MODIS C6 active fire data  
and mean-monthly GFWED precipitation (Fig. 3g) and temperature (Fig. 3i) variables were weaker compared to  
relationships among monthly NK MODIS C6 active fire data and mean-monthly GFWED relative humidity and DC  
variables (Fig. 3h, j). The level of significance varied among monthly NK MODIS C6 active fire data and mean-monthly  
180 GFWED precipitation correlations.

Precipitation and fire inverse relationships were even lower over NK than over Bolivia across all different precipitation  
estimates (Table 1). The strongest observed relationship for precipitation was between NK MODIS C6 and MERRA 2  
precipitation, with a 95% correlation confidence interval of -0.07 – -0.35. Next, a significant inverse relationship was  
observed between MODIS C6 active fire data and NK MERRA2 relative humidity, with a 95% correlation confidence



185 interval of -0.21 – -0.47. A positive relationship was seen among NK MODIS C6 active fire and MERRA2 temperature data, with a 95% correlation confidence interval of 0.24 – 0.49. Finally, significant relationships were found among NK MODIS C6 active fires and TRMM DC, GPCP DC, CPC DC, and MERRA 2 DC. Of the four DC, the MERRA2 DC had the weakest relationship to NK MODIS C6 active fires. The strongest relationship for DC was between MODIS C6 active fire data and TRMM DC, with a 95% correlation confidence interval of 0.39 – 0.61.

190

### 3.4 Spatial distribution of fire and DC

During 2010, fire was widespread (Fig. 4a) and September GPCP DC values were higher and spatially coherent in northeast Bolivia (Fig. 4b). During 2014, fire was less active in lowland Bolivia (Fig. 4c) and GPCP DC during September was lower than 2010 (Fig. 4d). Outside of NK, fire occurred in the cerrado, SDTF, METF and seasonally inundated wetland biomes (Fig. 4a, c). Within NK, 223 MODIS C6 active fires were observed in 2010 (Fig. 4a), and 17 MODIS C6 active fires were observed in 2014 (Fig. 4c). During both years, fires in NK occurred primarily in the cerrado biome on the Huanchaca Plateau.

195

### 3.5 Fire and forest loss

200 Forest loss from 2000–2012 (Fig. 5a) largely corresponded to areas where MODIS C6 fires occurred from 2001–2015 (Fig. 5b). Within NK, the majority of forest loss can be found on the Huanchaca plateau where the cerrado biome is found, along the cerrado-METF boundary, and in seasonally-inundated wetlands. Overall, forest loss is minimal within NK compared to the unprotected areas adjacent to NK (Fig. 5b). For unprotected areas outside of NK, forest loss occurred in the cerrado, SDTF, METF, and seasonally inundated wetland biomes, and in urban/agriculture land use zones (Fig. 5a). Forest loss outside of NK largely corresponded to areas where fire also occurred (Fig. 5b).

205

### 3.6 Using visibility data as a proxy of longer-term regional fire activity

Considering the positive relationship between lowland Bolivia MODIS C6 active fire data and mean-September  $B_{ext}$ , we use  $B_{ext}$  to extend the regional fire record for lowland Bolivia prior to the MODIS C6 record. Consistent with correlations among MODIS C6 fire and GFWED variables (Table 1), monthly correlations among  $B_{ext}$  and GFWED variables from 1/2001–12/2015, were significant (Table 2). However, correlations among  $B_{ext}$  and GFWED variables were slightly weaker when

210





compared to the same correlations using MODIS C6 fire data. Nevertheless, many relationships were significant. Based on these relationships,  $B_{\text{ext}}$  visibility data is used as a proxy of longer-term (i.e., 1982–2015) regional fire activity in lowland Bolivia (Fig. 6).

215 Over the longer record from 1982–2015, correlations among  $B_{\text{ext}}$  and GFWED variables were similar in strength to correlations among  $B_{\text{ext}}$  and GFWED variables from 2001–2015 (Table 2). In some cases, correlations strengthened over the longer record from 1982–2015, compared to the shorter record from 2001–2015 (e.g., correlation between  $B_{\text{ext}}$  and CPC DC). During the fire season (i.e., August–October) from 1982–2015,  $B_{\text{ext}}$  and GFWED regional-scale relationships in Bolivia (Table 3; Fig. 6) show consistency with previous results (Table 2; Fig. 3). In particular, the relationship between fire season  
220  $B_{\text{ext}}$  and MERRA2 temperature was not significant (Fig. 6c). Strongest relationships are observed among fire season  $B_{\text{ext}}$  and fire season GFWED DC and relative humidity variables (Fig. 6b, d).

## 4. Discussion

### 4.1 Drivers of fire in lowland Bolivia and NK

225 From 2001–2015, our analyses reveal strong fire seasonality in lowland Bolivia (Fig. 2a) and NK (Fig. 2b). Within NK, drought conditions were the main driver of fire (e.g., Table 1; Fig 3j), while fires in unprotected areas of lowland Bolivia were controlled by a combination of drought (e.g., Fig. 4a, 4c, 6d), biome type (e.g., Fig. 5), and forest loss likely influenced by human activities (Fig. 5b).

High fire years in 2004, 2007 and 2010 (Fig. 3a), correspond to years of drought (Chen et al., 2013b) and high fire years  
230 in the southern Amazon identified by others (Chen et al., 2013b; van Marle et al., 2017). Prolonged drought conditions in the southern Amazon are caused by reduced rainfall, higher-than-normal temperatures, and reduced atmospheric moisture during the wet and dry seasons (Marengo et al., 2008). Our results suggest the CPC DC and regional  $B_{\text{ext}}$  (Table 2; Fig. 3e, j) captured drought conditions that impacted the southern Amazon during the mid-1990's into the 2000's. In addition to high DC values, lower-than-normal relative humidity (Fig. 3c, h) and higher-than-normal temperature (Fig. 3d, i) were linked to  
235 increased fire activity in lowland Bolivia and NK (Table 1). Further demonstrating the connection between drought and fire in NK and lowland Bolivia were drought years and non-drought years, when fire was either significantly enhanced (Fig. 4a), or reduced (Fig. 4b). In particular, GPCP DC values were higher in lowland Bolivia during 2010, a high fire year (Fig. 4 a,



c), and GPCP DC values were lower during 2014, a low fire and DC year (Fig. 4 b, d). Our results are consistent with others who found synchronous changes in fire activity between tropical forest and cerrado biomes in the Amazon (Chen et al., 2013b). During 2014, fire in NK and the surrounding unprotected areas was significantly reduced across all biomes (Fig. 4b). The opposite occurred in 2010, when drought conditions and increased fire activity were observed across all biomes during the fire season (Fig. 4a, c).

While our results and paleosedimentary records (Burbridge et al., 2004; Maezumi et al., 2015) show fires are frequent on the cerrado landscape in NK (Killeen et al., 2002), whether drought, human activities, or a combination of both were the dominant drivers of recent fire activity in the SDTF and METF biomes in lowland Bolivia is less understood. Considering unfragmented tropical Amazon forests are more resilient to fire and drought conditions (Cochrane, 2003; Davidson et al., 2012) than fragmented tropical Amazon forests (Nepstad et al., 1999; Laurance and Williamson, 2001; Fearnside, 2005; Chen et al., 2013b), we suggest the spatial correspondence of forest loss and fire in METFs outside of NK (Fig. 5) was associated with forest clearing activities for economic practices common in the area (e.g., Killeen et al., 2008).

Seen as forest loss (Fig. 5b), the logging of Amazon forests has increased dry surface fuels, suppressed soil moisture, and created an environment susceptible to fire during drought (Nepstad et al., 1999; Fearnside, 2005; Chen et al., 2013a,b). Large geometric rectangular areas of forest loss observed in METFs and other biomes surrounding NK indicate forest loss from fire was not from lightning ignitions alone. However, an area of fire and forest loss seen in the METF west of NK appears spatially random, and not necessarily because of human activities alone. Further, spatial correspondence is observed in 2010, between fire, high DC (Fig. 4a, 4c) and forest loss in the METF biome west of NK, suggesting high DC was a dominant control on fire and forest loss in 2010. While we did not directly monitor human activities, our results suggest human activities further amplified forest loss and fire during high DC years. Spatial coherency between fire and forest loss seen in our results, and the results of others suggests fire in the SDTF and METF biomes is a function of human and lightning ignitions amplified by drought during the historical record (Killeen et al., 2002; Brown et al., 2006), and the paleorecord (Denevan, 1992; Bush et al., 2008).

#### 4.2 Fire relationship to different biomes



265 Fire within NK is a function of biome type (Fig. 1b, 4, 5). In NK, fires ignited by lighting are frequent in the cerrado biome from August–October (Killeen et al., 2002). Consistent with Cochrane (2003), a lack of fire activity was observed in the METF biome in NK from 2001–2015. Fire during the MODIS C6 record in lowland Bolivia and in NK was largely restricted to the cerrado and seasonally inundated wetland biomes.

Biome-boundary dynamics among the cerrado and other biomes influence fire in the southern Amazon (Power et al., 2016). Extreme seasonal droughts can amplify the role of fire on biome-boundaries among the cerrado, SDTF, and METF. The drying out plant biomass and soil moisture increases the potential for cerrado grassland fire propagation into neighboring biomes (Power et al., 2016). Amazon forest boundaries are vulnerable to positive feedbacks linked to forest loss and climate induced drought that increases forest fragmentation and fire propagation (Laurance and Williamson, 2001). Unprotected areas outside of NK show evidence of biome-boundary dynamics related to fire and forest loss (Fig. 5b). The majority of fires in the METF are observed at biome-boundary interfaces. Both boundary-biome dynamics and human caused forest loss seem to have impacted fire in the SDTF and METF biomes during our study.

275

### 4.3 $B_{\text{ext}}$ and GFWD relationship to fire in lowland Bolivia

We use  $B_{\text{ext}}$  visibility data to extend our regional fire signal from 1982–2015. We suggest high  $B_{\text{ext}}$  in 1987, 1988, 1995, and 1999 are indicative of increased fire activity (Fig. 6). The five lowest visibility (i.e., high  $B_{\text{ext}}$ ) years from 1982–2015, are observed towards the end of the visibility record in 1995, 1999, 2004, 2007, and 2010, corresponding to high MODIS C6 fire years in 2004, 2007, and 2010 (Fig. 3a). Our results are consistent with van Marle et al. (2017) who identified higher-than-normal particulate matter emitted into the atmosphere over the southwestern Amazon in 1988, 1995, 1999, 2004, 2007, and 2010. Consistency between our results and van Marle et al. (2017), suggests  $B_{\text{ext}}$  visibility, with limitations in mind (van Marle et al., 2017), can be used as a proxy of regional-fire activity for the southwestern Amazon and lowland Bolivia.

285 From 1982–2015, the strongest correlations (Table 3) were between mean fire season CPC DC (i.e., August–October) and mean fire season  $B_{\text{ext}}$  (i.e., August–October). The next strongest correlation was between mean fire season MERRA2 relative humidity and mean fire season  $B_{\text{ext}}$ . Our results suggest from 2001–2015, and from 1982–2015, regional fire activity in Bolivia responded to interannual CPC DC and relative humidity variability.



We speculate antecedent dry conditions linked to precipitation and temperature anomalies prior to the fire season impacted high DC values and fire in Bolivia and NK. When southern Amazon wet season drought is severe terrestrial water storage deficits can amplify drought and fire severity during the subsequent dry season (Chen et al., 2013a). Wet season drought leading to drought and fire seems plausible considering the DC is used here as an indicator of heavy-surface fuel drying over several months and deep, organic soil moisture content (Field et al., 2015). Further, this would explain weaker linear correlations observed among fire,  $B_{ext}$ , precipitation and temperature. We recommend future studies investigating climate and fire relationships in tropical and subtropical ecosystems use the DC as an indicator of antecedent dry conditions.

#### 4.4 Considerations and implications of GFWED and WMO-visibility data

Future studies should consider the DC sensitivity to the type of precipitation data used. DC values were less biased when using TRMM and GPCP precipitation, and demonstrated a strong correlation with MODIS C6 fire data for lowland Bolivia and NK (Table 1). MERRA2 DC and CPC DC values were consistently higher than TRMM DC and GPCP DC values for both lowland Bolivia and NK from 2001–2015. MERRA2 DC values exceeded 800 for lowland Bolivia and 1,000 for NK, much higher than TRMM and GPCP values.

In addition to the GFWED data used in our study, errors associated with the WMO-visibility data are important to consider. Visibility data are vulnerable to errors related to human-observed measurements, and are derived from spatially inconsistent weather stations distributed in the Amazon region (van Marle et al., 2017). Because of the role variable smoke transport has on relationships between fire activity and visibility, we have limited our visibility to only the broadest relationships across the large lowland area of Bolivia. We note, however, that the regional visibility signal was relatively insensitive to whether it was calculated from 4, 6, 8, or 11 stations (Fig. A1).

Given these limitation, our results demonstrate (i.e., 2001–2015) connections among fire in lowland Bolivia,  $B_{ext}$  variability (Fig. 2), interannual climate variability (Fig. 3, 4, 6), biome type (e.g., Fig. 4), forest loss (Fig. 5), and biome-boundary dynamics (e.g., Fig. 5). Future climate changes could impact drought severity and fire activity in lowland Bolivia. From 1979–1996, fire season length decreased, or did no change in lowland Bolivia (Jolly et al., 2015). However, from 1996–2013, fire season length increased in the Brazilian Amazon north and east of lowland Bolivia (Jolly et al., 2015), corresponding to a period of increased emissions in the southern Amazon (van Marle et al., 2017) and lowland Bolivia (Fig.



6). In the Amazon Basin, a projected increase in Fire Weather Index (FWI) is expected for period 2026–2045 (Bedia et al.,  
315 2015), and fire season severity is expected to increase during the 21<sup>st</sup> century (Flannigan et al., 2013). Projections of fire  
season length increasing, FWI increasing, and fire severity increasing (Flannigan et al., 2013) are of concern for lowland  
Bolivia when considering our results, and the impacts drought conditions have on increased fire activity in lowland Bolivia.  
We provide further understanding of how different biomes respond to drought and fire in lowland Bolivia, important when  
considering uncertainties regarding the fate of the Amazon (Zhang et al., 2015).

320 While increased FWI and fire severity are a concern for lowland Bolivia and for carbon emissions and global climate,  
fire leading to forest loss in the METF biome within NK was not observed from 2001–2015 (Fig. 2b, 4, 5). Our results  
suggest if human activities that amplify fire in the southern Amazon were restricted, recent fire activity could have been  
reduced in the METF biome. Considering the spatial distribution of fires in NK, and the spatial coherence of forest loss and  
fire in the unprotected METF biome outside of NK (Fig. 5b), a major limitation of our study is that we did not quantify the  
325 amount of forest loss in lowland Bolivia from human activities. As mentioned by others (e.g., Bedia et al., 2015), to better  
understand potential impacts of fire to southern Amazon tropical forests, human activities causing forest loss and fire need to  
be considered. To minimize forest loss from human deforestation and fire in the southern Amazon, our results and others  
(Flannigan et al., 2013) suggest human ignitions need to be reduced. Incentives and policies implemented in parts of the  
Brazilian Amazon (Nepstad et al., 2009) should be implemented in lowland Bolivia to reduce fire and forest loss in the  
330 METF biome, and to reduce smoke pollution that impacts carbon emissions and global climate.

## 5 Conclusions

We have demonstrated how multiple data can be used to explore relationships between climate, fire, land use, forest loss,  
and smoke emissions. A key finding, high DC and low humidity were dominant causes of recent fire activity in unprotected  
335 and protected areas of lowland Bolivia. In addition, fire was likely enhanced by fragmented biomes because of human  
activities, seen as forest loss in our results. Of interest to biogeographers, fires in NK from 2001–2015, occurred primarily in  
the cerrado biome and in seasonally inundated wetlands, and were absent from the NK METF biome with the exception of



cerrado–METF biome interfaces. Considering fire was minimal in the NK METF biome from 2001–2015, we recommend tropical forests in the southern Amazon and lowland Bolivia need further protection from human ignitions and deforestation.

340 In addition to exploring climate, fire, land use and biome relationships, we used  $B_{\text{ext}}$  visibility data to extend our regional fire record for lowland Bolivia prior to 2001. Our results and the results of others suggest visibility data can be used as a proxy of regional-fire activity in the southwestern Amazon and lowland Bolivia. We recommend future studies use WMO-visibility data to extend regional fire records.

#### 345 **Data Availability**

MODIS C6 data can be obtained at <https://earthdata.nasa.gov/earth-observation-data/near-real-time/firms/active-fire-data>. GFWED data is available at <https://data.giss.nasa.gov/impacts/gfwed/>. Data used to calculate horizontal visibility can be obtained from <https://catalog.data.gov/dataset/integrated-surface-global-hourly-data>. MODIS-based Global Land Cover Climatology data is available at [https://landcover.usgs.gov/global\\_climatology.php](https://landcover.usgs.gov/global_climatology.php). Global Forest Change Landsat data can  
350 be found at [https://earthenginepartners.appspot.com/science-2013-global-forest/download\\_v1.2.html](https://earthenginepartners.appspot.com/science-2013-global-forest/download_v1.2.html).

#### **Acknowledgments**

This material is based upon work supported by the National Science Foundation Graduate Research Fellowship under Grant 1256065. Any opinion, findings, and conclusions or recommendations expressed in this material are those of the authors(s)  
355 and do not necessarily reflect the views of the National Science Foundation. RF was supported by the NASA Precipitation Measurement Missions Science Team and the NASA Modeling, Analysis and Prediction Program.

#### **Appendices**

Figure. A1

#### 360 **References**

- Aragão, L. E., Malhi, Y., Roman-Cuesta, R. M., Saatchi, S., Anderson, L. O., Shimabukuro, Y. E.: Spatial patterns and fire response of recent Amazonian droughts, *Geophysical Research Letters*, 34, 2007.
- Aragão, L. E., Poulter, B., Barlow, J. B., Anderson, L. O., Malhi, Y., Saatchi, S., Phillips, O. L., Gloor, E.: Environmental  
365 change and the carbon balance of Amazonian forests, *Biological Reviews*, 89, 913–931, 2014.



- Asner, G. P., Alencar, A.: Drought impacts on the Amazon forest: the remote sensing perspective, *New Phytologist*, 187, 569–578, 2010.
- 370 Bedia, J., Herrera, S., Gutiérrez, J. M., Benali, A., Brands, S., Mota, B., Moreno, J. M.: Global patterns in the sensitivity of burned area to fire-weather: Implications for climate change, *Agricultural and Forest Meteorology*, 214, 369–379, 2015.
- Broxton, P. D., Zeng, X., Sulla-Menashe, D., Troch, P. A.: A Global Land Cover Climatology Using MODIS Data, *J. Appl. Meteor. Climatol.*, **53**, 1593–1605, <http://dx.doi.org/10.1175/JAMC-D-13-0270.1>, 2014.
- 375 Brown, I. F., Schroeder, W., Setzer, A., De Los Rios Maldonado, M., Pantoja, N., Duarte, A., Marengo, J.: Monitoring Fires in Southwestern Amazonia Rain Forests, *EOS Amer. Geophys. Union*, 87, 253–264, 2006.
- Burbridge, R. E., Mayle, F. E., Killeen, T. J.: Fifty-thousand-year vegetation and climate history of Noel Kempff Mercado  
380 National Park, Bolivian Amazon, *Quaternary Research*, 61, 215–230, 2004.
- Bush, M. B., Silman, M. R., McMichael, C., Saatchi, S.: Fire, climate change and biodiversity in Amazonia: a Late-Holocene perspective, *Philosophical Transactions of the Royal Society B: Biological Sciences*, 363, 1795–1802, 2008.
- 385 Chen, M., Shi, W., Xie, P. P., Silva, V. B. S., Kousky, V. E., Higgins, R. W., Janowiak, J. E.: Assessing objective techniques for gauge-based analyses of global daily precipitation, *J. Geophys. Res.*, 113, D04110, <http://dx.doi.org/10.1029/2007JD009132>, 2008.
- Chen, Y., Velicogna, I., Famiglietti, J. S., Randerson, J. T. Satellite observations of terrestrial water storage provide early  
390 warning information about drought and fire season severity in the Amazon, *Journal of Geophysical Research: Biogeosciences*, 118, 495–504, 2013a.
- Chen, Y., Morton, D. C., Jin, Y., Collatz, G. J., Kasibhatla, P. S., van der Werf, G. R., DeFries, R. S., Randerson, J. T.:  
395 Long-term trends and interannual variability of forest, savanna and agricultural fires in South America, *Carbon Manage.*, 4, 617–638, <http://dx.doi.org/10.4155/cmt.13.61>, 2013b.
- Cochrane, M. A.: Fire science for rainforests, *Nature*, 421, 913–919, <http://dx.doi.org/10.1038/nature01437>, 2003.
- 400 Cochrane, M. A., Barber, C. P.: Climate change, human land use and future fires in the Amazon, *Global Change Biology*, 15, 601–612, 2009.
- Davidson E. A., de Araújo, A. C., Artaxo, P., Balch, J. K., Brown, I. F., Bustamante, M. M., Coe, M. T., DeFries, R. S., Keller, M., Longo, M. and Munger, J. W.: The Amazon basin in transition, *Nature*, 481, 321–328, <http://dx.doi.org/10.1038/nature10717>, 2012.
- 405 de Groot W. J., Flannigan, M. D.: Climate change and early warning systems for wildland fire, In *Reducing Disaster: Early Warning Systems For Climate Change*, 127–151, 2014.
- Fearnside, P. M.: Deforestation in Brazilian Amazonia: history, rates, and consequences. *Conservation biology*, 19(3), 680–  
410 688, 2005.
- Field, R. D., van der Werf, G. R., Shen, S. S.: Human amplification of drought-induced biomass burning in Indonesia since 1960, *Nature Geoscience*, 2, 185–188, 2009.



- 415 Field, R. D., Spessa, A. C., Aziz, N. A., Camia, A., Cantin, A., Carr, R., de Groot, W. J., Dowdy, A. J., Flannigan, M. D.,  
Manomaiphiboon, K., Pappenberger, F., Tanipat, V., Wang, X.: Development of a Global Fire Weather database, *Nat.*  
*Hazards Earth Syst. Sci.*, 15, 1407–1423, <http://dx.doi.org/10.5194/nhess-15-1407-2015>, 2015.
- 420 Field, R. D., van der Werf, G. R., Fanin, T., Fetzer, E. J., Fuller, R., Jethva, H., Levy, R., Livesey, N., Luo, M., Torres, O.,  
Worden, H. M.: Indonesian fire activity and smoke pollution in 2015 show persistent nonlinear sensitivity to El Niño-  
induced drought, *Proceedings of the National Academy of Sciences*, 113, 9204–9209, 2016.
- 425 Gelaro, R., McCarty, W., Suárez, M. J., Todling, R., Molod, A., Takacs, L., Randles, C. A., Darmenov, A., Bosilovich, M.  
G., Reichle, R., and Wargan, K.: The Modern-Era Retrospective Analysis for Research and Applications, Version 2  
(MERRA2). *J. Climate*, 30, 5419–5454, 2017.
- Giglio, L., Shroeder, W., Justice, C. O.: The collection 6 MODIS active fire detection algorithm and fire products, *Remote  
Sensing of Environment*, 178, 31–41, 2016.
- 430 Hansen, M. C., Potapov, P. V., Moore, R., Hancher, M., Turubanova, S., Tyukavina, A., Thau, D., Stehman, S. V., Goetz, S.  
J., Loveland, T. R., and Kommareddy, A.: “High-Resolution Global Maps of 21st-Century Forest Cover Change”, *Science*  
342, 850–853, 2013.
- 435 Husar, R. B., Husar, J. D., Martin, L.: Distribution of continental surface aerosol extinction based on visual range  
data, *Atmospheric environment*, 34, 5067–5078, 2000.
- Huffman, G. J., Adler, R. F., Bolvin, D.T., Gu, G.: Improving the global precipitation record: GPCP Version 2.1, *Geophys.  
Res. Lett.*, 36, L17808, <http://dx.doi.org/10.1029/2009gl040000>, 2009.
- 440 Huffman, G. J., Adler, R.F., Bolvin, D. T., Gu, G., Nelkin, E. J., Bowman, K. P., Hong, Y., Stocker, E. F., Wolff, D. B.: The  
TRMM multisatellite precipitation analysis (TMPA): Quasiglobal, multiyear, combined-sensor precipitation estimates at fine  
scales, *Journal Hydrometeorology*, 8, 38–55, <http://dx.doi.org/10.1175/jhm560.1>, 2007.
- 445 Jolly, W. M., Cochrane, M. A., Freeborn, P. H., Holden, Z. A., Brown, T. J., Williamson, G. J., Bowman, D. M.: Climate-  
induced variations in global wildfire danger from 1979 to 2013, *Nature Communications*, 6, 2015.
- Killeen, T. J., Siles, T. M., Grimwood, T., Tieszen, L. L., Steininger, M. K., Tucker, C. J., Panfil, S.: Habitat heterogeneity  
on a forest–savannah ecotone in Noel Kempff Mercado National Park (Santa Cruz, Bolivia): implications for the long-term  
conservation of biodiversity in a changing climate, in: *How landscapes change: human disturbance and ecosystem  
450 fragmentation in the Americas*, vol.162, (Eds. Bradshaw, G. A., and Marquet P. A.), 285–312, 2002.
- Killeen T. J., Guerra, A., Calzada, M., Correa, L., Calderon, V., Soria, L., Quezada, B., Steininger, M. K.: Total historical  
land-use change in eastern Bolivia: Who, where, when, and how much?, *Ecology and Society* 13, 36, 2008.
- 455 Laurance, W. F., Williamson, G. B.: Positive feedbacks among forest fragmentation, drought, and climate change in the  
Amazon, *Conservation Biology*, 15, 1529–1535, 2001.
- Maezumi, S. Y., Power, M. J., Mayle, F. E., McLauchlan, K. K., Iriarte, J.: Effects of past climate variability on fire and  
vegetation in the cerrão savanna of the Huanchaca Mesetta, NE Bolivia, *Climate of the Past*, 11, 835–853,  
460 <http://dx.doi.org/10.5194/cp-11-835-2015>, 2015.
- Marengo, J. A., Nobre, C. A., Tomasella, J., Cardoso, M. F., Oyama, M. D.: Hydro-climatic and ecological behaviour of the  
drought of Amazonia in 2005, *Philosophical Transactions of the Royal Society of London B: Biological Sciences*, 363,  
1773–1778, 2008.





- 465 Marengo, J. A., Tomasella, J., Alves, L. M., Soares, W. R., Rodriguez, D. A.: The drought of 2010 in the context of historical droughts in the Amazon region, *Geophysical Research Letters*, 38, 2011.
- 470 Marlon, J. R., Bartlein, P. J., Carcaillet, C., Gavin, D. G., Harrison, S. P., Higuera, P. E., Joos, F., Power, M. J., and Prentice, I. C.: Climate and human influences on global biomass burning over the past two millennia, *Nature Geoscience*, 1, 697–702, 2008.
- 475 Mayle, F. E., Langstroth, R. P., Fisher, R. A., Meir, P.: Long-term forest–savannah dynamics in the Bolivian Amazon: implications for conservation, *Phil. Trans. R. Soc. B*, 362, 291–307, 2007.
- 480 Moran, E. F.: Deforestation and land use in the Brazilian Amazon, *Hum. Ecol.*, 21, 1–21, <http://dx.doi.org/10.1007/BF00890069>, 1993.
- 485 Morton, D. C., DeFries, R. S., Randerson, J. T., Giglio, L., Schroeder, W., van der Werf, G. R.: Agricultural intensification increases deforestation fire activity in Amazonia, *Global Change Biol.*, 14, 2262–2275, <http://dx.doi.org/10.1111/j.1365-2486.2008.01652.x>, 2008.
- 490 Morton, D. C., DeFries, R. S., Nagol, J., Souza, C. M., Kasischke, E. S., Hurtt, G. C., Dubayah, R.: Mapping canopy damage from understory fires in Amazon forests using annual time series of Landsat and MODIS data, *Remote Sensing of Environment*, 115, 1706–1720, 2011.
- 495 Morton, D. C., Le Page, Y., DeFries, R., Collatz, G. J., Hurtt, G. C.: Understory fire frequency and the fate of burned forests in southern Amazonia, *Philos. Trans. Roy. Soc. B*, 368, 20120163, <http://dx.doi.org/10.1098/rstb.2012.0163>, 2013.
- 500 Nepstad, D. C., Verssimo, A., Alencar, A., Nobre, C., Lima, E., Lefebvre, P., Schlesinger, P., Potter, C., Moutinho, P., Mendoza, E., Cochrane, M.: Large-scale impoverishment of Amazonian forests by logging and fire, *Nature*, 398, 505–508, 1999.
- 505 Nepstad, D., Soares-Filho, B. S., Merry, F., Lima, A., Moutinho, P., Carter, J., Bowman, M., Cattaneo, A., Rodrigues, H., Schwartzman, S., and McGrath, D. G.: The end of deforestation in the Brazilian Amazon, *Science*, 326, 1350–1351, 2009.
- 510 Power, M. J., Mayle, F. E., Bartlein, P. J., Marlon, J. R., Anderson, R. S., Behling, H., Brown, K. J., Carcaillet, C., Colombaroli, D., Gavin, D. G., and Hallett, D. J.: Climatic control of the biomass-burning decline in the Americas after AD 1500, *The Holocene*, 23, 3–13, 2013.
- 515 Power, M. J., Whitney, B. S., Mayle, F. E., Neves, D. M., de Boer, E. J., Maclean, K. S.: Fire, climate and vegetation relationships in the Bolivian Chiquitano seasonally dry tropical forest, *Phil. Trans. R. Soc. B*, 371, 20150165, 2016.
- 520 van der Werf, G. R., Randerson, J. T., Giglio, L., Collatz, G. J., Mu, M., Kasibhatla, P. S., Morton, D. C., DeFries, R. S., Jin, Y., van Leeuwen, T. T.: Global fire emissions and the contribution of deforestation, savanna, forest, agricultural, and peat fires (1997–2009), *Atmos. Chem. Phys.*, 10, 11707–11735, <http://dx.doi.org/10.5194/acp-10-11707-2010>, 2010.
- 525 van Marle, M. J. E., van der Werf, G. R., de Jeu, R. A. M., Liu, Y. Y.: Annual South American forest loss estimates based on passive microwave remote sensing (1990–2010), *Biogeosciences*, 13, 609, 2016.
- 530 van Marle, M. J. E., Field, R. D., Werf, G. R., Estrada de Wagt, I. A., Houghton, R. A., Rizzo, L. V., Artaxo, P., Tsigaridis, K.: Fire and deforestation dynamics in Amazonia (1973–2014). *Global Biogeochemical Cycles*, 31, 24–38, 2016.



515 World Meteorological Organization: Guide to Meteorological Instruments and Methods of Observation, 6<sup>th</sup> ed., Secretariat of the World Meteorological Organization, Geneva, Switzerland, 1996.

Wooster, M. J., Zhukov, B., Oertel, D.: Fire radiative energy for quantitative study of biomass burning: Derivation from the BIRD experimental satellite and comparison to MODIS fire products, *Remote Sensing of Environment*, 86, 83–107, 2003.

520 Zhang, K., Almeida Castanho, A. D., Galbraith, D. R., Moghim, S., Levine, N. M., Bras, R. L., Coe, M. T., Costa, M. H., Malhi, Y., Longo, M., and Knox, R. G.: The fate of Amazonian ecosystems over the coming century arising from changes in climate, atmospheric CO<sub>2</sub>, and land use, *Global change biology*, 21, 2569–2587, 2015.

525 **Table 1.** Mean monthly Pearson's correlations (01/2001 – 12/2015) between Moderate Resolution Imaging Spectroradiometer 6 (MODIS C6) active fires  $\geq 90\%$  confidence, and Global Fire WEather Database (GFWED) variables for Bolivia (i.e. table columns 1-2) and NK (i.e. table columns 3-4). All correlation p-values were  $< .001$  with 178 degrees of freedom, unless otherwise noted (e.g., NK MODIS and MERRA2 precipitation: p-value = .003). Correlations are listed in order of strongest (i.e. top row) to weakest (i.e. bottom row).

| <b>Bolivia</b>                           | 95% Confidence Interval | <b>NK</b>  | 95% Confidence Interval |
|--|-------------------------|--|-------------------------|
| Bolivia MODIS & GCPC DC                  | 0.69 – 0.82             | NK MODIS & TRMM DC                                 | 0.39 – 0.61             |
| Bolivia MODIS & TRMM DC                  | 0.68 – 0.81             | NK MODIS & GCPC DC                                 | 0.38 – 0.60             |
| Bolivia MODIS & CPC DC                   | 0.65 – 0.79             | NK MODIS & CPC DC                                  | 0.33 – 0.56             |
| Bolivia MODIS & MERRA2 DC                | 0.58 – 0.74             | NK MODIS & MERRA2 DC                               | 0.28 – 0.53             |
| Bolivia MODIS & MERRA2 relative humidity | -0.56 – -0.73           | NK MODIS & MERRA2 temperature                      | 0.24 – 0.49             |
| Bolivia MODIS & MERRA2 temperature       | 0.43 – 0.64             | NK MODIS & MERRA2 relative humidity                | -0.21 – -0.47           |
| Bolivia MODIS & MERRA2 precipitation     | -0.27 – -0.51           | NK MODIS & MERRA2 precipitation (*p-value = 0.003) | -0.07 – -0.35           |
| Bolivia MODIS & GCPC precipitation       | -0.25 – -0.50           | NK MODIS & GCPC precipitation (*p-value = 0.004)   | -0.07 – -0.35           |
| Bolivia MODIS & TRMM precipitation       | -0.24 – -0.50           | NK MODIS & TRMM precipitation (*p-value = 0.004)   | -0.06 – -0.34           |
| Bolivia MODIS & CPC precipitation        | -0.24 – -0.49           | NK MODIS & CPC precipitation (*p-value = 0.01)     | -0.05 – -0.33           |

530 **Table 2.** Mean monthly Pearson's correlations (01/2001 – 12/2015) between Bext(km-1), and Global Fire WEather Database (GFWED) variables for Bolivia (i.e., table columns 1-2), compared to the same Pearson's correlations over the



535

entire GFWED record from 01/1982 to 12/2015 (i.e., table columns 3-4). All correlation p-values were  $< 0.001$ , unless otherwise noted (e.g., Bext(km<sup>-1</sup>) and MERRA2 precipitation: \*p-value = 0.0013). Bolivia (01/2001 – 12/2015) correlations have 178 degrees of freedom, and Bolivia (01/1982 – 12/2015) correlations have 406 degrees of freedom respectively. Correlations (i.e., table columns 1-2) are listed in order of strongest (i.e. top row) to weakest (i.e. bottom row).

| <b><u>Bolivia (01/2001 – 12/2015)</u></b>                          | 95% Confidence Interval | <b><u>Bolivia (01/1982 - 12/2015)</u></b>          | 95% Confidence Interval |
|--|-------------------------|--|-------------------------|
| Bext(km <sup>-1</sup> ) & TRMM DC                                  | 0.38 – 0.60             | N/A  | N/A                     |
| Bext(km <sup>-1</sup> ) & GCPC DC                                  | 0.37 – 0.60             | N/A  | N/A                     |
| Bext(km <sup>-1</sup> ) & CPC DC                                   | 0.34 – 0.57             | Bext(km <sup>-1</sup> ) & CPC DC                   | 0.45 – 0.59             |
| Bext(km <sup>-1</sup> ) & MERRA2 DC                                | 0.33 – 0.56             | Bext(km <sup>-1</sup> ) & MERRA2 DC                | 0.36 – 0.52             |
| Bext(km <sup>-1</sup> ) & MERRA2 relative humidity                 | -0.24 – -0.49           | Bext(km <sup>-1</sup> ) & MERRA2 relative humidity | -0.38 – -0.53           |
| Bext(km <sup>-1</sup> ) & MERRA2 temperature                       | 0.24 – 0.49             | Bext(km <sup>-1</sup> ) & MERRA2 temperature       | 0.33 – 0.49             |
| Bext(km <sup>-1</sup> ) & MERRA2 precipitation (*p-value = 0.0013) | -0.09 – -0.37           | Bext(km <sup>-1</sup> ) & MERRA2 precipitation     | -0.16 – -0.35           |
| Bext(km <sup>-1</sup> ) & GCPC precipitation (*p-value = 0.004)    | -0.07 – -0.35           | N/A  | N/A                     |
| Bext(km <sup>-1</sup> ) & TRMM precipitation (*p-value = 0.005)    | -0.07 – -0.35           | N/A  | N/A                     |
| Bext(km <sup>-1</sup> ) & CPC precipitation (*p-value = 0.007)     | -0.06 – -0.34           | Bext(km <sup>-1</sup> ) & CPC precipitation        | -0.17 – -0.35           |

540



545 **Table 3.** Mean fire season (i.e., August–October) Pearson’s correlations (01/1982–12/2015) between Bext(km<sup>-1</sup>), and Global Fire WEather Database (GFWED) variables for lowland Bolivia. All correlation p-values were < 0.001, unless otherwise noted.

| <b>Bolivia</b>  | 95% Confidence Interval |
|---|-------------------------|
| Bext(km <sup>-1</sup> ) & CPC DC                                  | 0.36 – 0.79             |
| Bext(km <sup>-1</sup> ) & MERRA2 relative humidity                | -0.25 – -0.74           |
| Bext(km <sup>-1</sup> ) & MERRA2 DC (*p-value = 0.007)            | 0.13 – 0.68             |
| Bext(km <sup>-1</sup> ) & MERRA2 precipitation (*p-value = 0.014) | -0.10 – -0.66           |
| Bext(km <sup>-1</sup> ) & CPC precipitation (*p-value = 0.046)    | -0.008 – -0.61          |
| Bext(km <sup>-1</sup> ) & MERRA2 temperature (*p-value = 0.13)    | -0.08 – 0.55            |

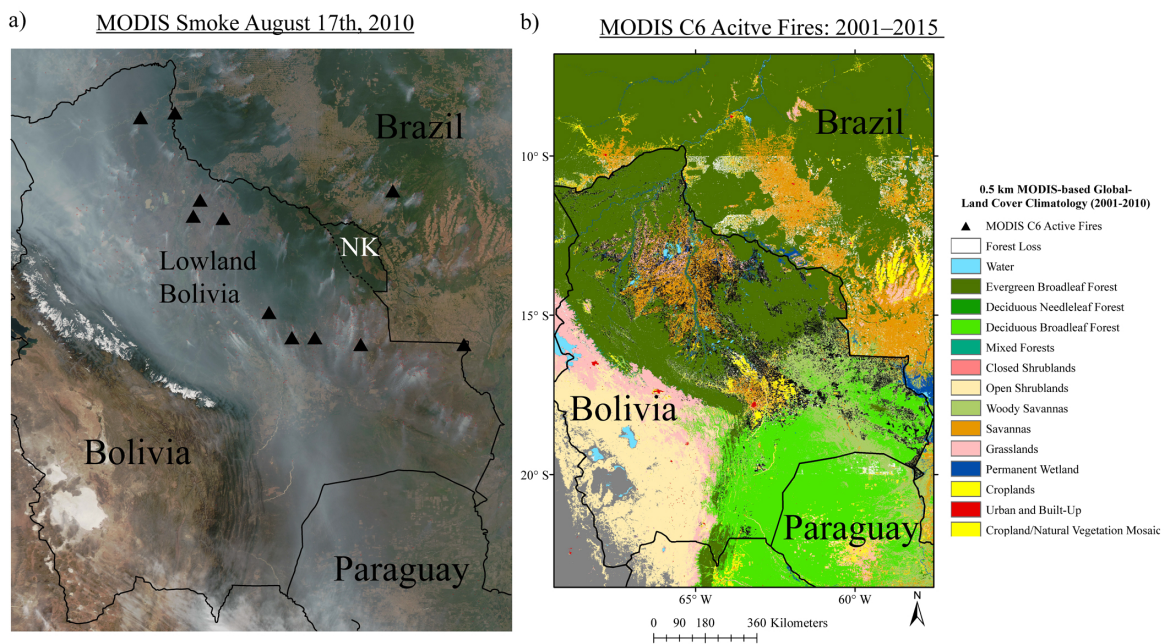


**Figure 1.** Fires and smoke observed by Moderate Resolution Imaging Spectroradiometer (MODIS) over Bolivia and Noel Kempff Mercado National Park (NK) on August 17th, 2010 (a), the highest fire year observed by the MODIS active fire product for Bolivia during the record (2001–2015). The locations of the eleven World Meteorological Organization (WMO)-level surface stations used to obtain visibility data are shown as black triangles (a). NASA image courtesy: Jeff Schmaltz. Forest loss from 2000–2012 (Hansen et al., 2013) displayed as white (b), and Moderate Resolution Imaging Spectroradiometer C6 (MODIS C6) active fires  $\geq 90\%$  confidence from 2001–2015, displayed as black triangles (b). MODIS based Collection 5.1 MCD12Q global land cover data [Broxton et al., 2014] is included (b).

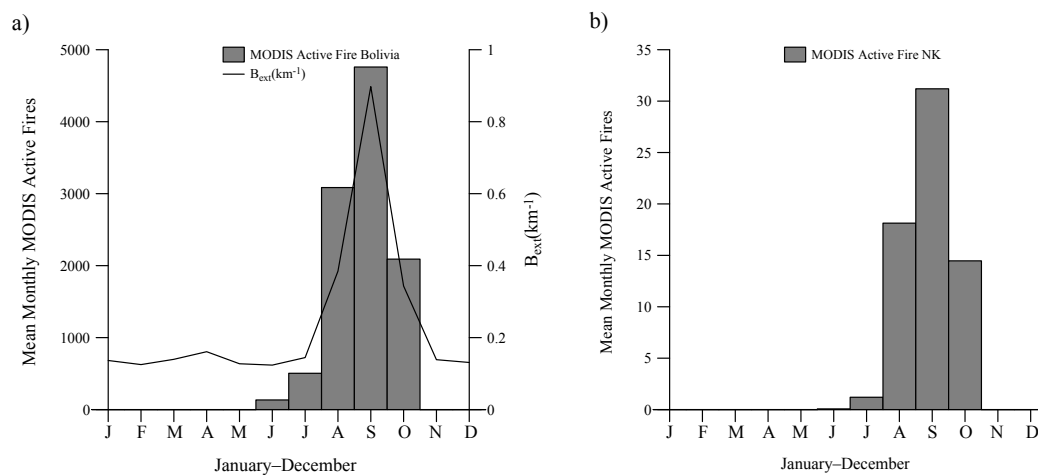


**Figure 2.** Mean-monthly Moderate Resolution Imaging Spectroradiometer 6 (MODIS 6) active fires  $\geq 90\%$  confidence (2001–2015) for Bolivia (a) and Noel Kempff Mercado National Park (NK) (b). Mean-monthly extinction coefficient ( $B_{ext} \text{ km}^{-1}$ ) (1973–2015) is included for Bolivia (a). Fire seasonality is clearly demonstrated for both Bolivia (a) and NK (b) (e.g. peak fire from August–October). For Bolivia, 85% of fires were detected from August–October (MODIS 6 active fire  $\geq 90\%$  confidence). For NK, 96% of fires were detected from August–October (MODIS 6 active fire  $\geq 90\%$  confidence). From 2001–2015, a 95% correlation confidence interval of 0.76 – 0.86, was observed between mean-monthly  $B_{ext} \text{ km}^{-1}$  and monthly lowland Bolivia MODIS C6 active fires (a).

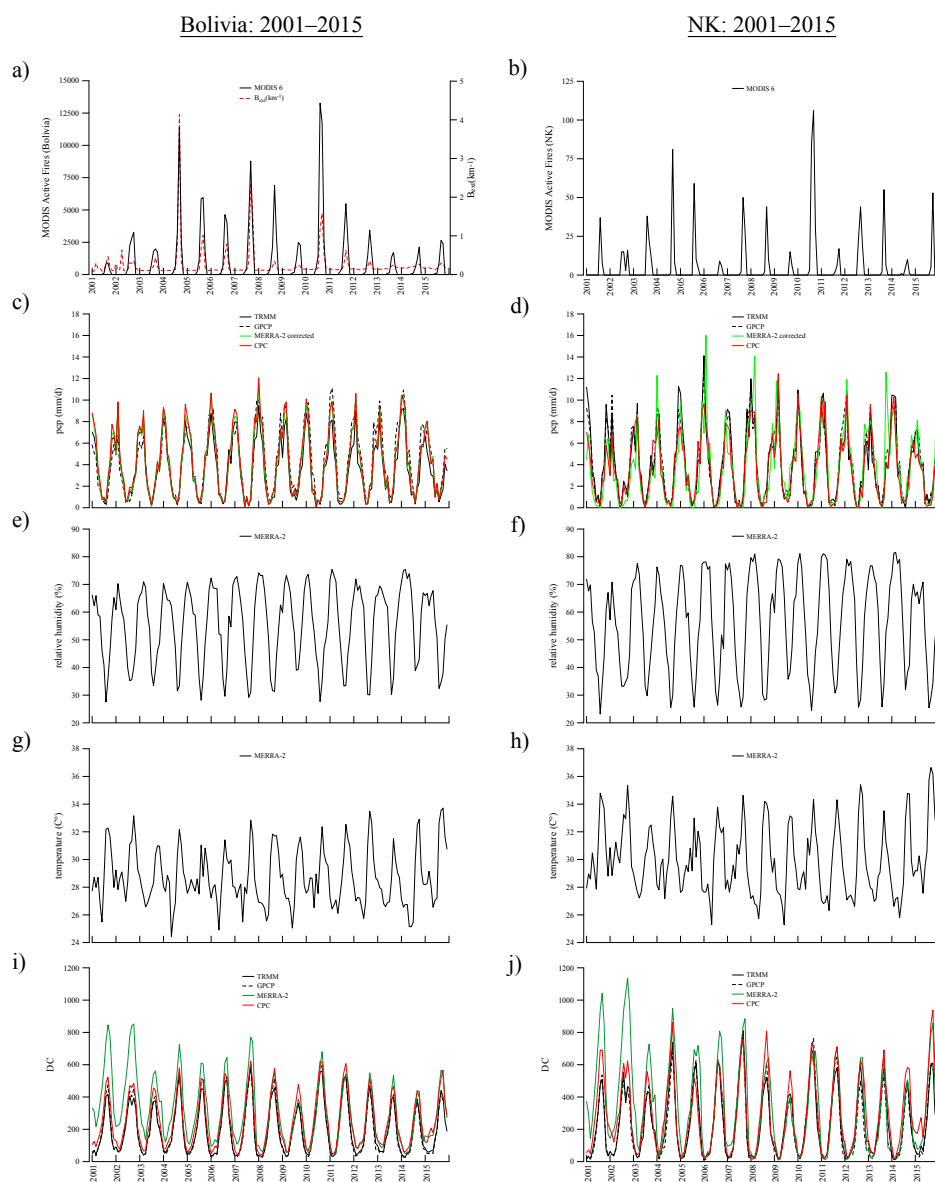


**Figure 3.** Mean-monthly (Jan–Dec) timeseries of MODIS C6 active fires (a,b), of the extinction coefficient  $B_{ext}$  (a), and of selected Global Fire Weather Database (GFWED) variables (c–j). Timeseries are for Bolivia (a,c,e,g,i) and NK (b,d,f,h,j) from 2001–2015. GFWED variables include precipitation from four sources (c,d), MERRA-2 relative humidity (e,f), MERRA-2 temperature (g,h), and the drought code (DC) calculated from four sources (i,j).

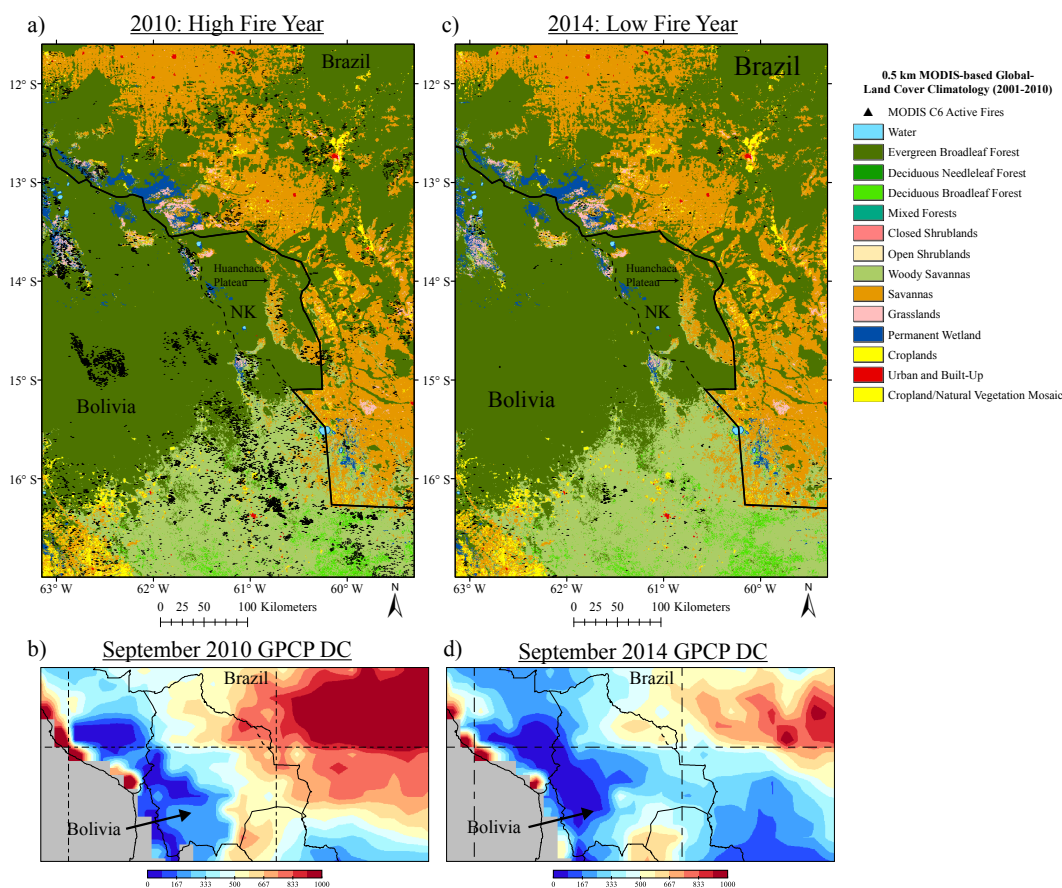


**Figure 4.** Moderate Resolution Imaging Spectroradiometer C6 (MODIS C6) active fires  $\geq$  90% confidence during 2010, a high fire year (a), and during 2014, a low fire year (c). September GPCP drought code (DC) during 2010 (b) and 2014 (d). MODIS based Collection 5.1 MCD12Q global land cover data [Broxton et al., 2014] is included. Noel Kempff Mercado National Park (NK) is the area that falls within the dotted-black polyline and the Bolivia-Brazil border.





MODIS C6 Active Fires: 2001–2015 and Forest Loss:  
 2000–2012

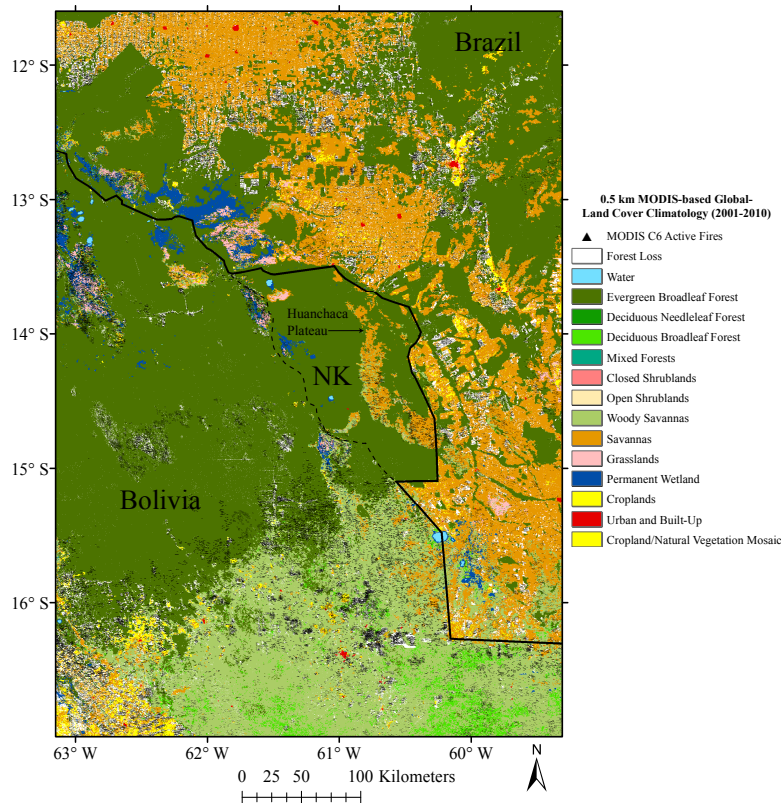


**Figure 5.** Forest loss from 2000–2012 (Hansen et al., 2013) displayed as white (a), and Moderate Resolution Imaging Spectroradiometer C6 (MODIS C6) active fires  $\geq$  90% confidence from 2001–2015 (b). MODIS based Collection 5.1 MCD12Q global land cover data [Broxton et al., 2014] is included. NK is the area that falls within the dotted-black polyline and the Bolivia-Brazil border.



Lowland Bolivia 1982–2015

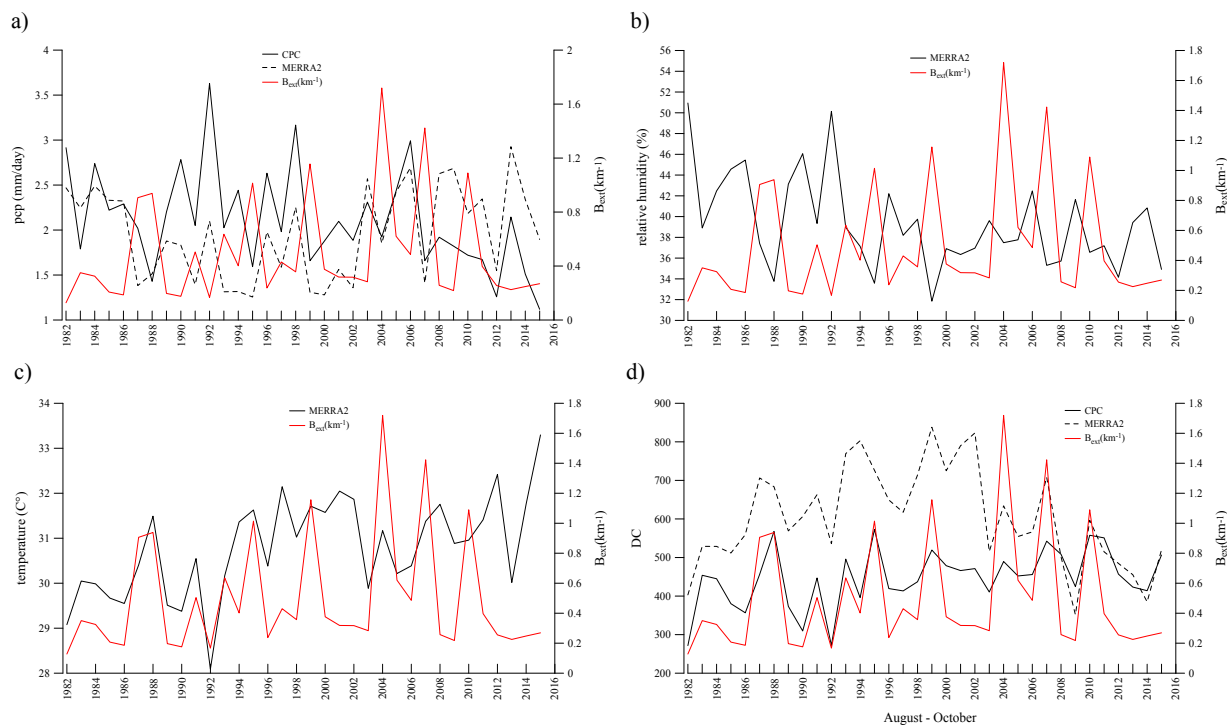


**Figure 6.** Mean fire season (Aug–Oct) time series (1982–2015) of daily Global Fire Weather Database (GFWD) variables for Bolivia including MERRA2 precipitation (a), MERRA2 relative humidity (b), MERRA2 temperature (c), and CPC and MERRA2 DC (d).  $B_{ext}$  ( $\text{km}^{-1}$ ) is included in each plot (i.e., red line).

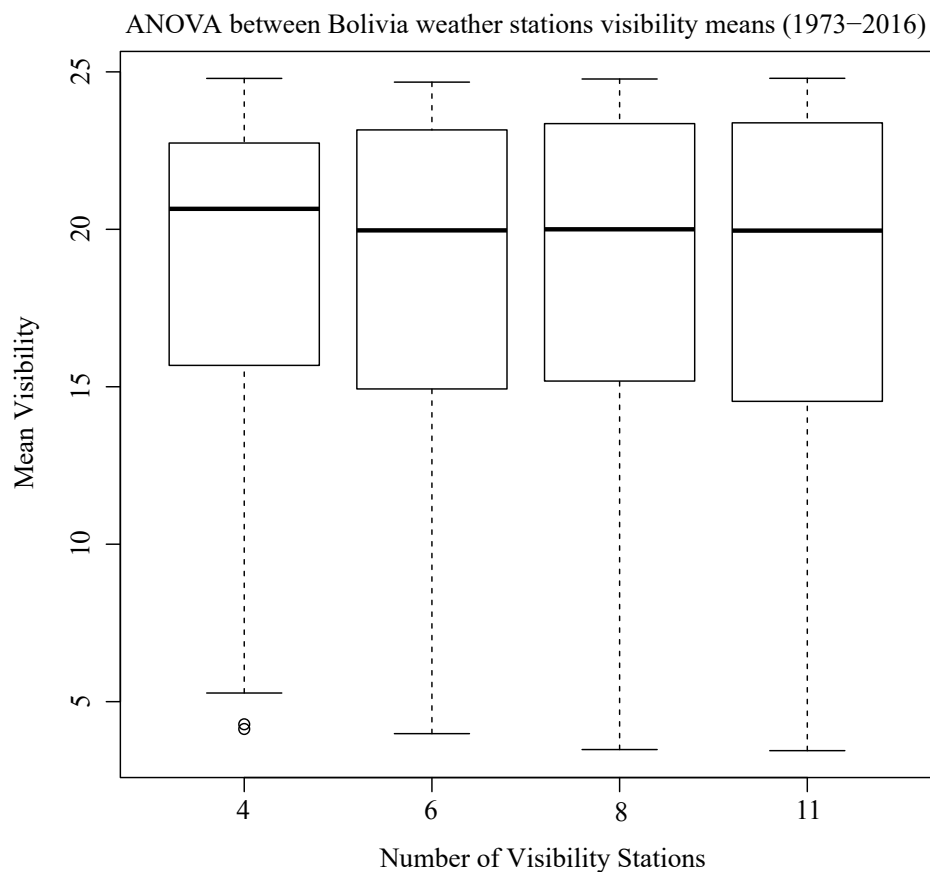


**Figure A1.** An ANOVA test was performed between four mean-monthly visibility timeseries (01/1973 - 12/2015) to explore variation between sample means. The mean-monthly visibility timeseries are derived from 4 stations, 6 stations, 8 stations, and 11 stations in Bolivia. Both the boxplot and an low F-statistic of .464 indicate the group means are very similar, and therefore increasing or decreasing the number of weather stations did not significantly change mean-monthly visibility data.